Inductance correction in impedance studies of solid oxide fuel cells

G. Raikova[1]*, P. Carpanese[2], Z. Stoynov[1], D. Vladikova[1], M. Viviani[3], A. Barbucci[2]

[1] *Institute of Electrochemistry and Energy Systems, Bulgarian Academy of Sciences,*
Acad. G. Bonchev St., Block 10, 1113 Sofia, Bulgaria
[2] *DICheP, Universita Di Genova, P. Le Kenedi 1, 16129 Genova, Italy*
[3] *CNR, IENI, V. De Marini 6, 16149, Genova, Italy*

A procedure for evaluation and elimination of errors, caused by parasitic inductance and resistance in EIS studies of two solid oxide fuel cells (SOFC) materials: yttria stabilized zirconia (YSZ) electrolyte and lanthanum strontium manganite (LSM)/YSZ composite cathode is presented in this paper. It is shown that for these low impedance systems the parasitic inductance can affect not only the high frequencies but also the middle and low ones. The parasitic errors correction procedure increases significantly the reliability of the electrochemical impedance spectroscopy (EIS) results.

Key words: electrochemical impedance spectroscopy (EIS), parasitic inductance error correction, yttria stabilized zirconia (YZS), composite lanthanum strontium manganite\yttria stabilized zirconia (LSM\YSZ) cathode.

INTRODUCTION

The complexity of the cathode and anode reactions processes at the triple phase boundary (gas/solid/solid), as well as the ionic-conductivity of the electrolyte in solid oxide, require new approaches for optimization of their performance. The Electrochemical Impedance Spectroscopy is emerging as one of the most powerful, informative and promising techniques, which combines the advantages of the methods, elucidating the knowledge about the electrochemical kinetics of the processes based on assessment of the general cell's behaviour.

The new generation high frequency response analyzers work in a wide frequency range (1 mHz – 50 MHz), which ensures simultaneous study of phenomena with big differences in the rates and in the time-constants. However, for low impedance systems, such as SOFCs, the direct application of EIS encounters the problem of the errors caused by the parasitic inductance. It originates basically from the nature of the objects under study, from the configuration of the measurement cell, including the cables connected with the electrochemical interface, which introduce also a parasitic resistance error. The parasitic inductance can influence not only the high frequencies but also the middle and low ones.

The theoretical analysis and topology simulation show that the errors caused by the parasitic inductance: (i) limit the measurement frequency; (ii) lead to inaccurate parametric identification; (iii) deform the impedance diagram [1–5]. Thus, the correct model recognition requires an accurate estimation of the parasitic inductance influence on the measured impedance.

It has been found [1, 4, 6–8] (Eqn. 1) that the inductance error ε_L is proportional to the square of the frequency (ω) and it depends on the values of the object's inductance (L) and of the capacitance (C_m), which are specific properties of the object:

$$\varepsilon_L = \frac{Z_{im}^L - Z_{im}}{Z_{im}} = -\omega^2 L C_m \quad , \quad (1)$$

where Z_{im}^L is the imaginary component of the system's impedance and Z_{im} is the imaginary component of an ideal system with zero inductance.

For large systems with high impedance the error is dominated by the capacitance [1, 4, 9]. For low impedance systems, such as SOFCs, the error is dominated by the inductance [1, 2, 9, 10].

Figures 1 and 2 represent structural deformations of some simple models, caused by the inductance influence. At low inductance values the complex plan impedance diagram of a Faradaic reaction is similar to that of an inductance free model (Fig. 1). With the increase of the inductance the capacitive semicircle, typical for this model, changes its size and shape drastically. The capacitive loop disappears and only the imaginary component of the main semi-circle remains, indicating that the Faradaic process is entirely hidden by the influence of the inductance.

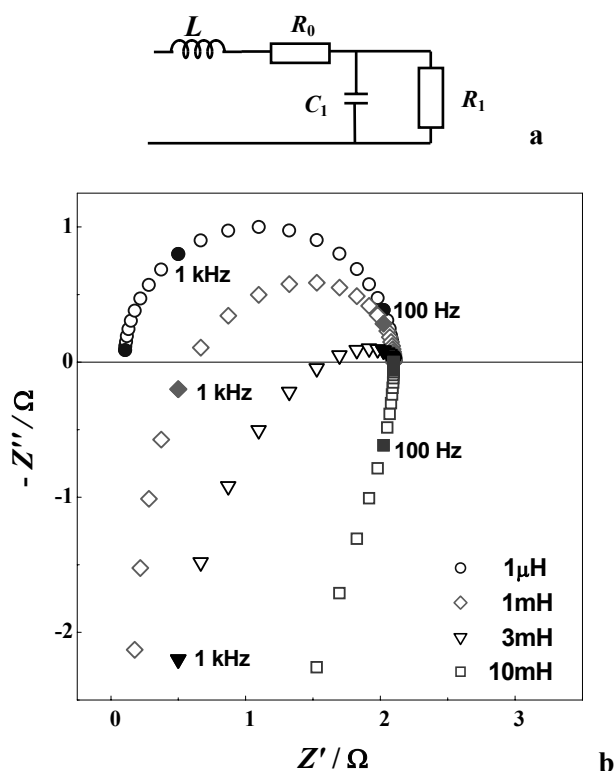* To whom all correspondence should be sent:
E-mail: graikova@bas.bg

Fig. 1. A model of simple Faradaic reaction ($R_0 = 0.1$ Ω; $C_1 = 10^{-3}$ F; $R_1 = 2$ Ω): a) Equivalent circuit; b) Complex plane impedance diagrams at different values of L.
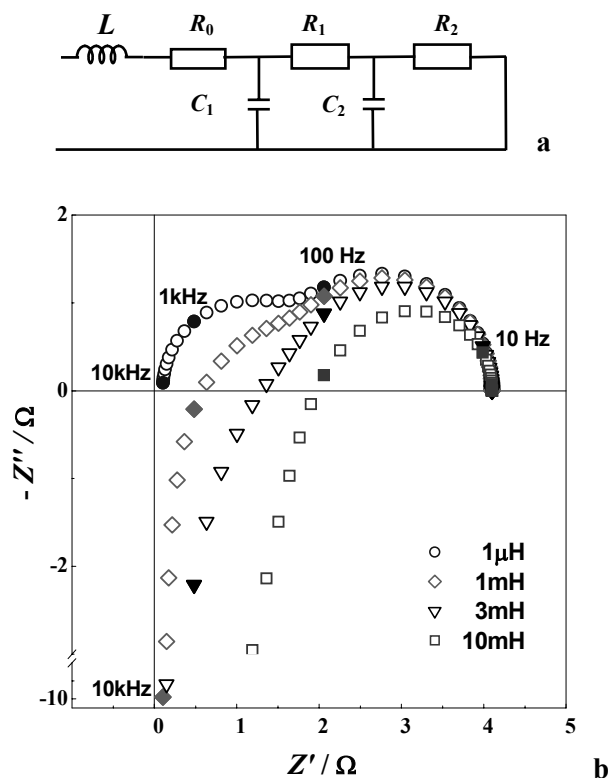

Fig. 2. A model of two-step Faradaic reaction involving one adsorbed spesies ($R_0 = 0.1$ Ω; $C_1 = 10^{-3}$ F; $R_1 = 2$ Ω; $C_2 = 0.01$ F; $R_2 = 2$ Ω): a) Equivalent circuit; b) Complex plane impedance diagrams at different values of L.

The results for a more complicated model of a two-step reaction are similar (Fig. 2). At lower inductance values, the deformation influences the high frequency semicircle. With the increase of L the first loop disappears and the deformation of the impedance shape resembles that of one step reaction (Fig. 2b).

The theoretical analysis of the errors shows that the influence of the parasitic inductance can be reduced by optimization of the cell's configuration and the sample's shape and size. Thus, when it is possible, the impedance measurements of objects with very low resistance, such as SOFCs, have to be carried out with small experimental cells, ensuring small electrode's surface area and thus smaller C_m (Eqn. (1)).

The deformed zones of the impedance diagrams, caused by parasitic inductance, often include significant information about the investigated object or phenomenon, which cannot be analyzed properly. The simple elimination of the inductive tail or the performance of measurements at lower initial frequencies [12] cannot solve the problem.

There are two main approaches for elimination of the parasitic inductance and resistance errors. The first one is to perform the identification procedure including terms for the cell's inductance and resistance in the hypothetical model (this approach cannot eliminate the difficulty to predict the correct model in the presence of strongly deformed diagram). The second approach is to perform calibration procedures in the same frequency range, followed by extraction of the parasitic components for every frequency. Since the first approach can be applied only for lumped elements, the second one could be regarded as a more general solution [1, 4, 5]. This paper presents a method for correction of the parasitic inductance, based on calibration measurements and its application to impedance characterization of materials for SOFCs.

EXPERIMENTAL

Impedance measurements

The impedance measurements of YSZ electrolyte were performed on single crystal samples produced by ESCETF Single Crystal Technology B.V, containing 8.5 mol% Y_2O_3. They had a square form with side length 10 mm and thickness 0.5 mm. Platinum electrodes were first painted onto both faces of the sample and then sintered in air at 900°C for 120 min [4, 8, 12–14]. The impedance measure-

ments were carried out on Solartron 1260 FRA in the frequency range 13 MHz – 0.1 Hz with density 9 points per decade. The amplitude of the a.c. signal was 50 mV. The measurements were performed in the temperature range from 200 to 950°C, in air atmosphere, at 50°C intervals. Before each measurement the sample was allowed to equilibrate thermally for 1 hour. For reduction of the cabling self-inductance, the components of the measuring system were connected externally by coaxial cables and the connecting leads were as short as possible.

The measurements of the composite cathode material (LSM/YSZ) were performed on three-electrode half-cells with an apparent cathode surface area of 0.23 cm² and thickness of 50 μm. More information about the cell's construction is given in [15–17]. The impedance measurements were carried out in air in the temperature interval between 400 and 900°C using an alumina-based rig with shielded Pt wires. A frequency response analyzer Solartron 1260 and an electrochemical interface (Solartron 1186) were used. The measurements were performed within the frequency range 0.1 Hz–50 kHz with amplitude of the a.c. signal 10 mV.

Calibration and inductance errors correction procedure

The performed calibration and correction procedure includes the following steps:
- Short circuit measurement. It serves for evaluation of the cell's inductance and resistance, including that of the cabling. The cathode and anode contacts of the cell are connected in a short circuit. This measurement is performed at the experimental frequency and in the temperature range.
- Measurement of a dummy object. This measurement, serves for evaluation of the sample's

self-inductance and resistance. It is carried out using a highly conducting (metal) dummy object with shape and dimensions identical to those of the real one. In the case of fuel cells, which are working at high temperatures (700–1000°C), the melting point of the metal has to be taken into consideration.
- Measurement of the investigated object (in the cell).
- Correction of the impedance measured at every frequency. This procedure is performed under the assumption that the impedance of the object and of the parasitic components are additive quantities.

RESULTS AND DISCUSSION

Calibration studies

In comparison with the impedance diagram of a simulated inductance model (Fig. 3a), the Nyquist's plot of the short circuit measurements obtained with the cell for YSZ studies (Fig. 3b) exhibit a "pipe" shaped form [4, 8, 14]. Its shift from the zero point determines the internal resistance of the cabling. This result shows that (i) the inductance of the cell and of the cabling is frequency dependent and (ii) the calibration determines both the parasitic inductance and resistance of the experimental configuration.

It is important to note that changes in the cables' length and configuration (for instance presence of a single loop) strongly influence the impedance and consequently the short circuit calibration measurement (Fig. 4.)

The comparison of a short circuit measurement of the experimental cell and of the external cable is given in Figure 5. The impedance of the cell at short circuit is shifted to the right with respect to that of the cable, due to the cell's parasitic resistance.
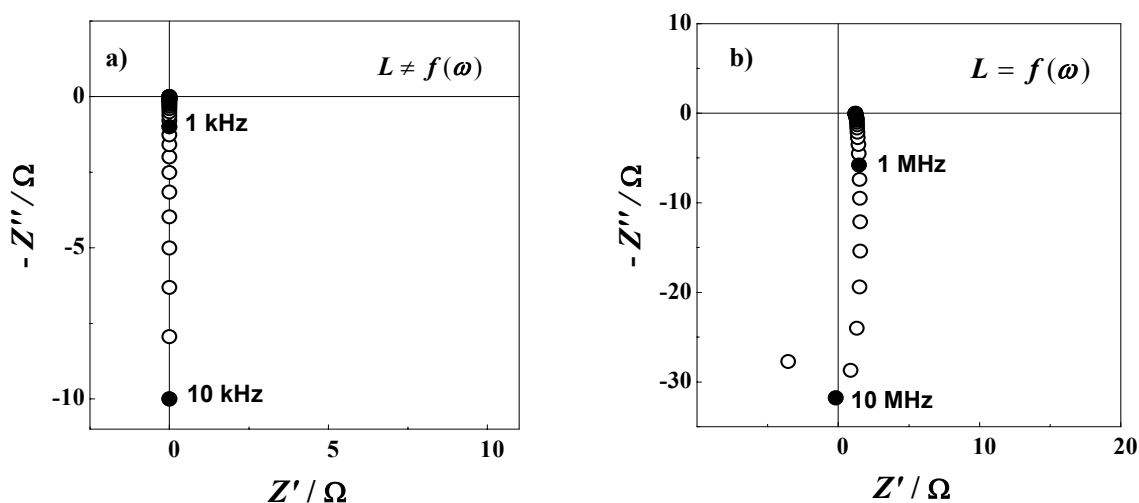
Fig. 3. Complex plane impedance diagram of: a) simulated inductance model (L=10H); b) calibration short circuit measurement of YSZ experimental cell.
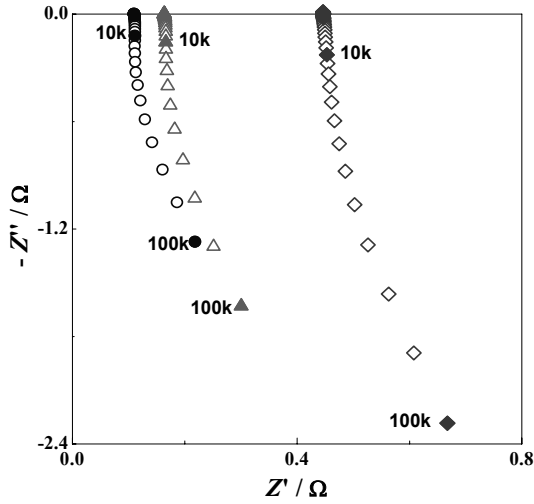
Fig. 4. Complex plane impedance diagram of the cabling: (○) cable with 80 cm length; (△) cable with the same length in the presence of a loop; (◇) cable with 130 cm length.
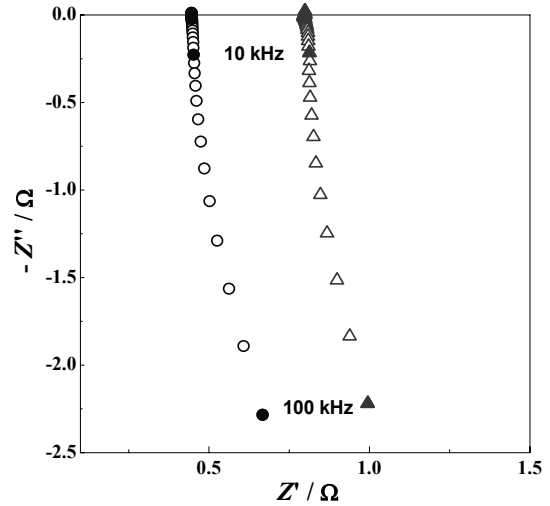

Fig. 5. Complex plane impedance diagram of the cabling (○) and of short circuit calibration measurement (△) of LSM/YSZ experimental cell.

Figure 6 represents the calibration measurements of a dummy object - brass disk with dimensions of the YSZ sample. Obviously, the difference between the cell's and the objects' inductance is negligible and its influence can be neglected.
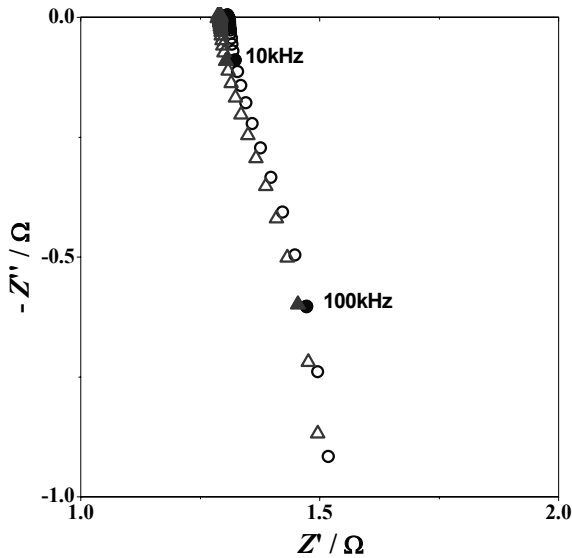

Fig. 6. Zoomed high frequency part of impedance diagrams of short circuit measurements (△) and of a dummy object (○).

Since the short circuit impedance is temperature dependent (Fig. 7), the performance of calibration measurements at each working temperature improves additionally the accuracy of the inductance errors' correction procedure.

The analysis of the calibration measurements shows that they have to be carried out with fixed configuration of the measurement cell and cables, which should remain unchanged in the course of the experiment.

Inductance errors correction in impedance studies of YSZ electrolyte

The high frequency inductance pipe-shaped "tail" in the impedance diagrams of YSZ appears at temperatures above 450°C (Fig. 8).

The characteristic frequency ω_L, at which the inductive and capacitive parts of the imaginary component becomes equal [4], determines the high frequency intercept with the real axis:

$$\omega_L L - \frac{\omega_L^2 R\tau}{1 + \omega_L^2 \tau^2} = 0 , \qquad (2)$$

where $\tau = RC$ is the time-constant.

In this example ω_L does not change with the temperature T:

$$\omega_L \approx \sqrt{1/LC_{eff}} \neq f(T) , \qquad (3)$$

where C_{eff} is the effective capacitance of the system.

The procedure for correction of the inductance and resistance errors was performed on the basis of the assumption that the impedance of the object and of the parasitic components are additive. It has been applied to every working temperature.
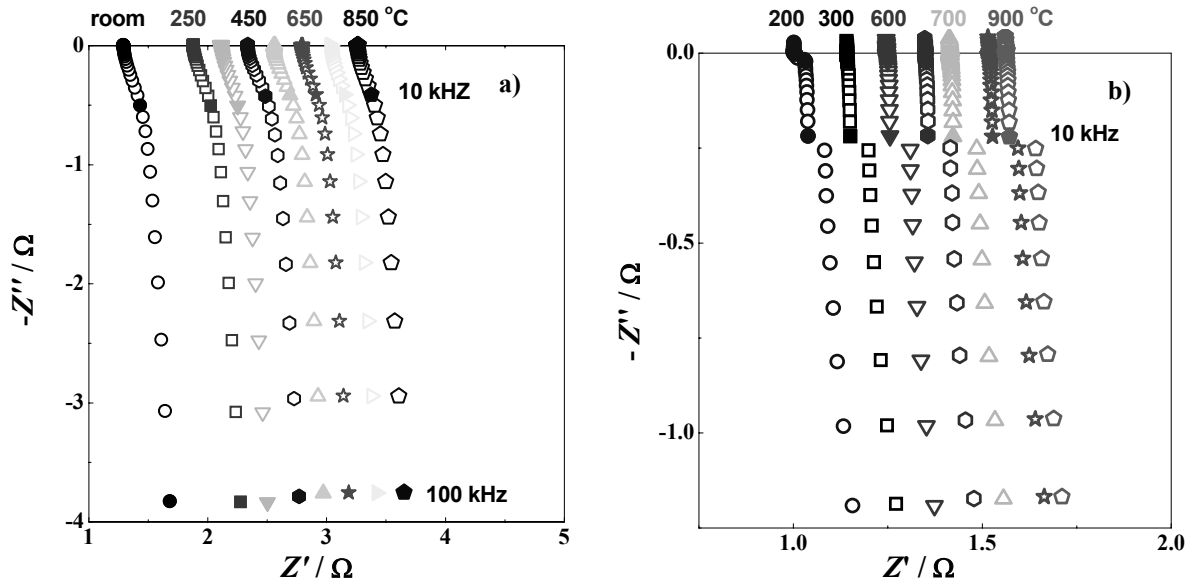
Fig. 7. Complex plane impedance diagrams of short circuit calibration measurements at different temperatures of: (a) cell for YSZ studies; (b) cell for LSM/YSZ studies.
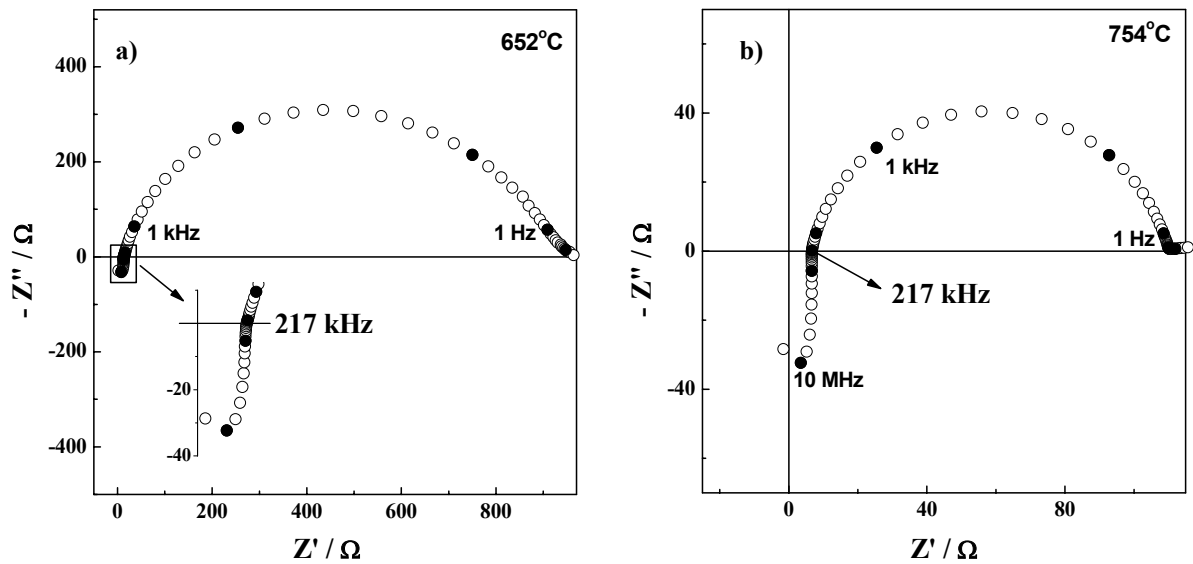

Fig. 8. Complex plane impedance diagrams of YSZ electrolyte measured at different temperatures (data before *L*-correction).

Figure 9 illustrates the correction procedure for YSZ single crystal sample at 838°C: calibration measurement at short circuit (Fig. 9a), measurement of the cell with the sample (Fig. 9b), correction of the sample's impedance for the cell's parasitic inductance and resistance at each working frequency (Fig. 9c, d).

The comparison of the impedance data obtained at higher temperatures before and after the parasitic errors correction shows (Fig. 10) that the deformations affect not only the high, but also the lower frequency range. Part of the first semicircle, which represents the resistance of the bulk material, is well visible even at the highest temperatures due to the correction.

The high frequency intercept with the real axis shifts toward smaller values after the correction (Figs. 9d, 10). The procedure increases the accuracy of determination of the electrolyte resistances. The inductance influences also the electrode reaction behaviour, which is revealed in the low frequency region. After the correction the estimated polarization resistance decreases (Fig. 10).

The estimated parasitic inductance of the investigated YSZ sample is about 7 nH.
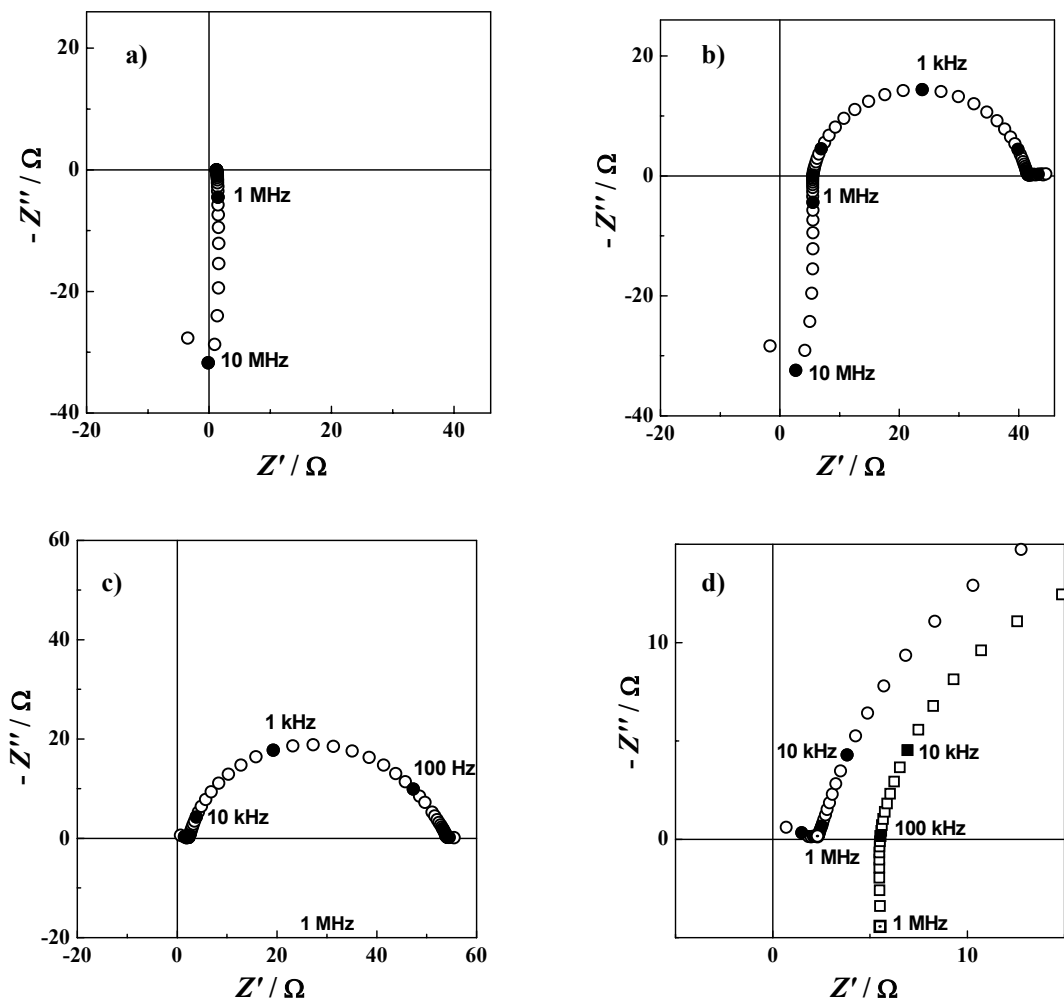
203

Fig. 9. Correction procedure for impedance of YSZ single crystal sample measured at 838°C.
Complex plane impedance diagrams of: a) short circuit measurement; b) sample's measurement;
c) sample's impedance after the correction; d) zoomed high frequency part of b) and c).
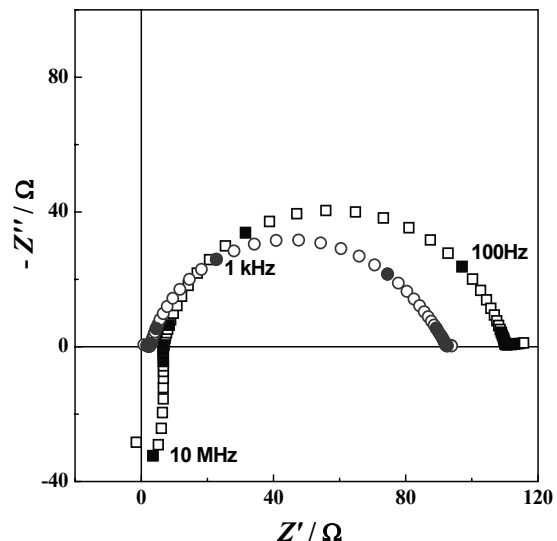

Fig. 10. Complex plane impedance diagrams for YSZ at
793ºC: (□) raw impedance data; (○) data after the errors
correction

*Inductance errors correction in impedance studies
of LSM/YSZ cathode material*

The inductive "tail" in the impedance diagrams
of LSM/YSZ composite cathode appears at 690°C
(Fig. 11). In this object ω_L is temperature dependent,
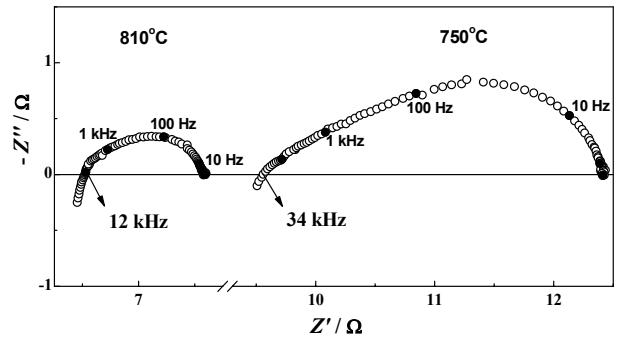which could be attributed to C_{eff} (Eqn. (3)).

Fig. 11. Complex plane impedance diagram of composite
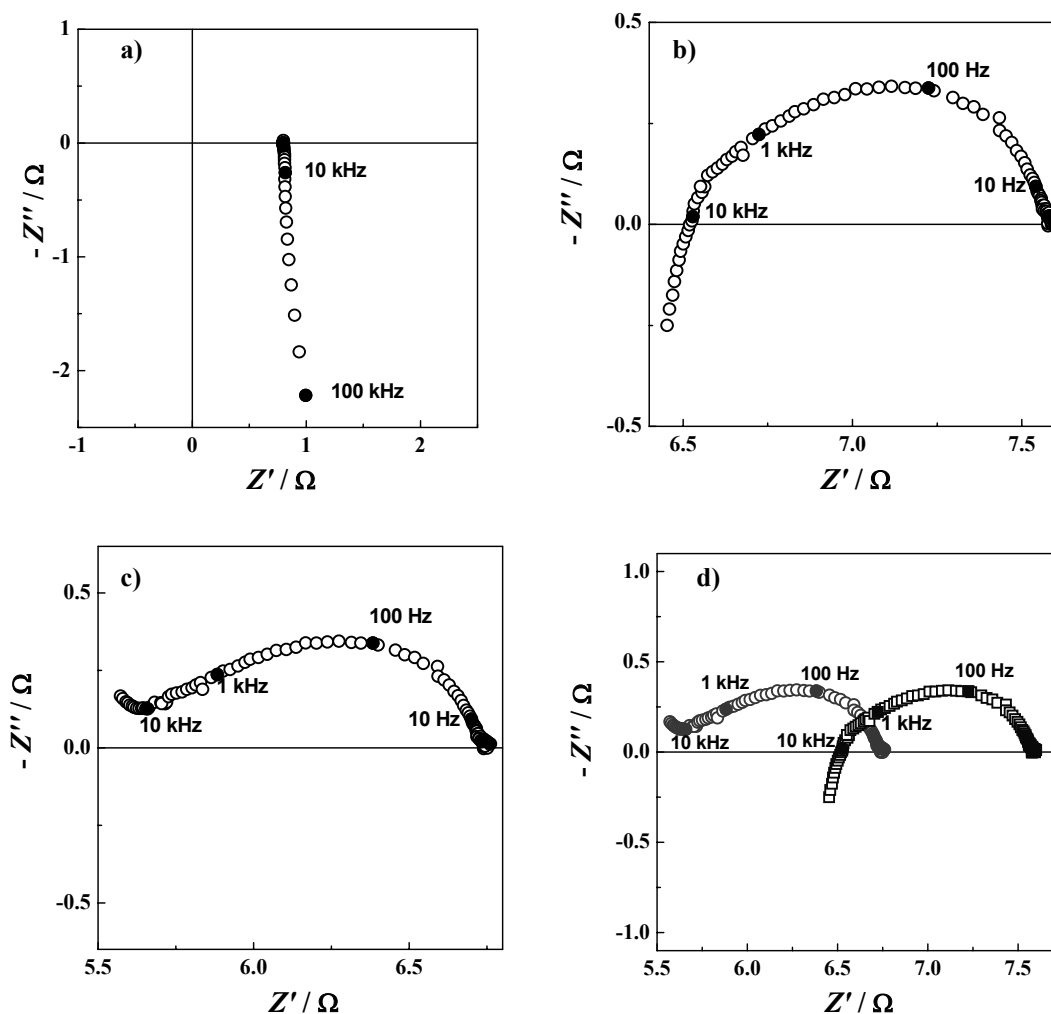LSM/YSZ cathode material at different temperatures.

Fig. 12. Correction procedure for the LSM/YSZ sample measured at 840°C. Complex plane impedance diagrams of: a) short circuit measurement; b) sample's impedance raw data; c) sample's impedance after the correction; d) comparison of impedance data before (□) and after (○) the errors correction.

The procedure of the parasitic inductance (and resistance) correction is represented in Figure 12. The comparison of the impedance diagrams before and after the correction (Figs. 12d, 13) indicates that for this system the errors influence mainly the higher frequencies (50–1 kHz). After the correction, the high-frequency inductance "tail" is replaced by a section of a semicircle, which represents the response of the electrolyte (Fig. 13).

The errors influence also the high-frequency region of the response related to the cathode reaction behaviour (10–1 kHz), i.e. the "left" part of the lower frequency arc (Fig. 13). While the raw data describe a depressed semicircle at this segment, the corrected ones follow a more linear shape. This difference can affect an eventual modeling procedure.

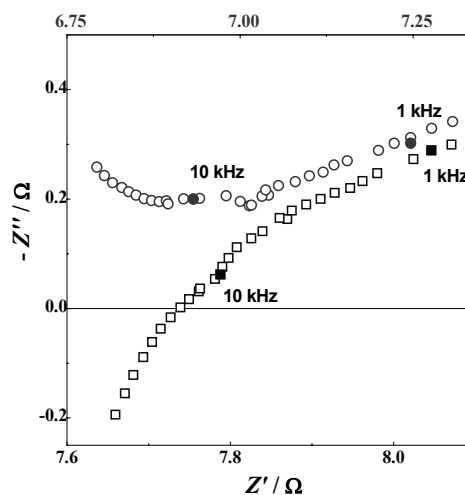The evaluated parasitic inductance for the investigated LSM/YSZ sample is about 4 nH.

Fig. 13. Comparison of the zoomed high-frequency parts of the complex plain impedance diagrams of LSM/YSZ sample measured at 780°C before (□) and after (○) the errors correction.

CONCLUSIONS

The correction of the parasitic inductance and resistance increases the informational capability of the impedance experimental data. The herein presented impedance studies of yttria stabilized zirconia solid electrolyte and LSM/YSZ composite cathode materials show the importance of the calibration measurements. The fixed configuration of the cell, cables and whole set-up during the experiments ensure reproducible impedance data. The results demonstrate the high accuracy, obtained by applying the parasitic errors correction procedure, which can be used for impendance studies of low resistance systems.

REFERENCES

1. B. Savova-Stoynov, Z. Stoynov, *J. Appl. Electrochem.*, **17**, 1150 (1987).
2. Z. Stoynov in: Materials for Lithium-Ion Batteries, C. Julien, Z. Stoynov (Eds.), Kluwer Academic Publishers, 2000, p. 349.
3. Z. Stoynov, B. Grafov, B. Savova-Stoynova, V. Elkin, Electrochemical Impedance, Nauka, Moscow, 1991 (in Russian).
4. D. Vladikova, Z. Stoynov, G. Raikova, in: Portable and Emergency Energy Sources, Z. Stoynov, D. Vladikova (Eds.), Marin Drinov Academic Publishing House, Sofia, 2006, p. 383.
5. Z. Stoynov, D. Vladikova, Differential Impedance Analysis, Marin Drinov Academic Publishing House, Sofia, 2005.
6. Z. Stoynov, B. Savova-Stoynova, T. Kossev, *J. Power Sources*, **30**, 275 (1990).
7. D. Vladikova, http://accessimpedance.iusi.bas.bg, Impedance Contributions Online, 1 (2003) L3-1; *Bulg. Chem. Commun.*, **36**, 29 (2004).
8. D. Vladikova, Z. Stoynov, G. Raikova, http://accessimpedance.iusi.bas.bg, Impedance Contributions Online, 3 (2005) P8-1; *Bulg. Chem. Commun.*, **38**, 226 (2006).
9. M. Keddam, Z. Stoynov, H. Takenouti, *J. Appl. Electrochem.*, **7**, 539 (1977).
10. Z. Stoynov, B. Savova-Stoynova, T. Kossev, *J. Power Sources*, **30**, 301 (1990).
11. S. B. Adler, *Solid State Ionics*, **135**, 603 (2000).
12. G. Raikova, D. Vladikova, J. A. Kilner, S. J. Skinner, Z. Stoynov, http://accessimpedance.iusi.bas.bg, Impedance Contributions Online, 2 (2004) P8–1; *Bulg. Chem. Commun.*, **37**, 46 (2005).
13. D. Vladikova, G. Raikova, Z. Stoynov, H. Takenouti, J. Kilner, S. J. Skinner, *Solid State Ionics*, **176**, 2005 (2005).
14. D. Vladikova, J. Kilner, S. J. Skinner, G. Raikova, Z. Stoynov, *Electrochim. Acta*, **51**, 1611 (2006).
15. A. Barbucci, M. Viviani, P. Carpanese, D. Vladikova, Z. Stoynov, *Electrochim. Acta*, **51**, 1641 (2006).
16. A. Barbucci, M. Viviani, P. Carpanese, D. Vladikova, Z. Stoynov, http://accessimpedance.iusi.bas.bg, Impedance Contributions Online, 4 (2006) P4-1; *Bulg. Chem. Commun.*, **39**, 203 (2007).
17. D. Vladikova, Z. Stoynov, A. Barbucci, M. Viviani, P. Carpanese, G. Raikova, in: New Developments in Advanced Functional Ceramics 2007, L. Mitoseriu (Ed.), Transworld Research Network, Kerala, India, 2007, p. 457.

КОРЕКЦИЯ НА ИНДУКТИВНИ ГРЕШКИ В ИМПЕДАНСНИ ИЗСЛЕДВАНИЯ НА ТВЪРДООКИСНИ ГОРИВНИ КЛЕТКИ

Г. Райкова[1]*, П. Карпанезе[2], З. Стойнов[1], Д. Владикова[1], М. Вивиани[3], А. Барбучи[2]

[1] *Институт по електрохимия и енергийни системи, Българска академия на науките, ул. „Акад. Г. Бончев", бл. 10, 1113 София*
[2] *Факултет по инженерна химия, Университет Генуа, пл. „Кенеди" № 1, 16129 Генуа, Италия*
[3] *Институт за енергетика, Национален изследователски център, ул. „Де Марини" № 6, 16149, Генуа, Италия*

(Резюме)

Предложена е процедура за оценка и отстраняване на грешки, причинени от паразитни индуктивност и съпротивление, при импедансни изследвания на два материала за твърдоокисни горивни клетки (SOFC): итриево-стабилизиран циркониев оксид електролит (YSZ) и композитен катод на базата на лантан-стронциев манганит/итриево-стабилизиран циркониев оксид (LSM/YSZ). Показано е, че при такива ниско-импедансни системи паразитната индуктивност може да повлияе не само на високочестотната, но също така на средно- и нискочестотната зона. Процедурата за корекция и отстраняване на грешки от паразитна индуктивност повишава значително надеждността на резултатите получени с електрохимичната импедансна спектроскопия (ЕИС).